



Water-soluble ions and oxygen isotope in precipitation over a site in northeastern Tibetan Plateau, China

Linqing Wang^{1,2} · Zhenxing Shen^{1,2} · Di Lu¹ · Hongmei Xu¹ · Ningning Zhang² · Yali Lei¹ · Qian Zhang³ · Xin Wang⁴ · Qiyuan Wang² · Junji Cao²

Received: 13 November 2018 / Accepted: 27 May 2019 / Published online: 17 June 2019
© Springer Nature B.V. 2019

Abstract

A total of 30 precipitation samples were collected at a remote site of Qinghai Lake in the northeastern Tibetan Plateau, China, from June to August 2010. All samples were analyzed for major cations (NH_4^+ , Na^+ , K^+ , Ca^{2+} , and Mg^{2+}) and anions (F^- , Cl^- , NO_3^- , and SO_4^{2-}), electric conductivity (EC), pH, dissolved organic carbon (DOC), and oxygen isotopic composition ($\delta^{18}\text{O}$). The volume-weighted mean (VWM) values of pH and EC in the precipitation samples were 7.2 and $19.0 \mu\text{s cm}^{-1}$. Ca^{2+} was the dominant cation in precipitation with a VWM of $116.9 \mu\text{eq L}^{-1}$ ($1.6\text{--}662.9 \mu\text{eq L}^{-1}$), accounting for 45.7% of total ions in precipitation. SO_4^{2-} was the predominant anion with a VWM of $32.7 \mu\text{eq L}^{-1}$, accounting for 47.1% of the total anions. The average precipitation DOC was 1.4 mg L^{-1} , and it shows a roughly negative power function with the precipitation amount. The values of $\delta^{18}\text{O}$ in the rainwater in Qinghai Lake varied from -13.5‰ to -3.9‰ with an average of -8.1‰ . The enrichment factor analysis indicates that crustal materials from continental dust were the major sources for Ca^{2+} in the precipitation samples. The high concentration of Ca^{2+} in the atmosphere played an important role in neutralizing the acidity of rainwater in Qinghai Lake area. Cluster analysis of air-mass trajectories indicates that the air masses associated with northeast and east had high values of NH_4^+ , SO_4^{2-} , and NO_3^- , whereas large Ca^{2+} loading was related to the air mass from west.

Keywords Precipitation chemistry · Water-soluble ions · Dissolved components · Enrichment factor · Qinghai Lake

✉ Zhenxing Shen
zxshen@mail.xjtu.edu.cn

¹ Department of Environmental Science and Engineering, Xi'an Jiaotong University, Xi'an 710049, China

² State Key Laboratory of Loess and Quaternary Geology, Institute of Earth Environment, Chinese Academy of Sciences, Xi'an 710075, China

³ School of Environmental & Municipal Engineering, Xi'an University of Architecture and Technology, Xi'an 710055, China

⁴ Multiphase Chemistry Department, Max Planck Institute for Chemistry, 55128 Mainz, Germany

1 Introduction

With the rapid urbanization and industrialization, excessive pollutants (e.g., sulfur dioxide (SO_2), nitrogen oxides (NO_x), volatile organic compounds (VOCs), and particulate matter (PM)) have emitted into the atmosphere in China (Shen et al. 2009; Zhang et al. 2015). These air pollutants can partly dissolve in precipitation and then remove from the atmosphere to the earth surface through wet deposition (Wright et al. 2018). Precipitation has been considered as one of the most effective pathways for scavenging atmospheric pollutants from the atmosphere (Seinfeld and Pandis 2016). Rainfall that contains a lot of pollutants would cause a series of negative environmental issues, such as acid rain, soil acidification, aquatic eutrophication, biodiversity reduction, and even global climate change (www.wmo.int/pages/prog/arep/gaw/precip_ch_em.html). The acidity and alkalinity of precipitation depend on the chemical species in rainwater, which is influenced by the emission sources for pollutants as well as their physical and chemical transformation (Cangemi et al. 2017; Nadzir et al. 2017; Shen et al. 2012; Xiao et al. 2013; Rao et al. 2016).

Qinghai Lake is located on the northeastern Tibetan Plateau, and it is the largest inland salt water lake in China. Due to its remote location, Qinghai Lake is an important natural laboratory for the environmental sciences chemistry and geochemistry (An et al. 2012; Meng et al. 2013; Zhang et al. 2014a; Wang et al. 2014). The mass concentration of atmospheric total suspended particulate was $41.5 \mu\text{g m}^{-3}$, and it may be influenced by anthropogenic sources from eastern China (Zhang et al. 2014a). Generally, there are two distinct seasons around the Qinghai Lake, that is, the wet season (or Asian monsoon season, June–September) and dry season (or non-monsoon season, October–April) (Tang 1998). Most of the precipitations occur during summer monsoon, with moisture originating from the Indian and Pacific Oceans (Li et al. 2007). Its lands are either arid or semi-arid, with frequent windy days (Wang et al. 2015). Recent researches focused on snow and ice chemistry in high elevation regions of Tibetan Plateau (Kang et al. 2010; Qian et al. 2015; Li et al. 2017a, 2017b; Yao et al. 2012). For example, Yang et al. (2012) investigated the chemical characteristics of precipitation at Shigatse, southern Tibetan Plateau, and found that HCO_3^- and Ca^{2+} were the major anion and cation ions detected in the samples, respectively; Zhang et al. (2012a) collected precipitation samples at Nam Co, central Tibetan Plateau, and indicated that crustal aerosol contributed largely to the loadings of Ca^{2+} , Mg^{2+} , SO_4^{2-} , and HCO_3^- in the rainwater samples, while lake salt was a major source for K^+ and Cl^- ; Zhang et al. (2014b) reported that crustal dust sources contributed 61%–85% of Ca^{2+} , Mg^{2+} , and K^+ in the rainwater while anthropogenic sources accounted for 68%–79% of SO_4^{2-} , NO_3^- , and NH_4^+ in Lijiang, southeast Tibetan Plateau. However, there are still limited studies on elevation regions precipitation chemistry, including chemical composition and the source analytical on the Tibetan Plateau. In this study, rainfall samples were collected during June to August 2010 in Qinghai Lake, and the water-soluble ions, DOC and $\delta^{18}\text{O}$ were also determined which can further help us understand the chemical properties of precipitations in the Tibetan Plateau. Thus, the purposes of this study were to characterize the chemical composition and to identify the possible sources of various constituents in precipitation in this region.

2 Methodology

2.1 Sampling site

A total of 30 precipitation samples were collected at the “bird island” peninsula (36.98°N, 99.88°E, 3200 m a.s.l.), which is located at the northwest section of the Qinghai Lake shore as shown in Fig. 1. Most of the precipitations in this island were occurred from June to October. There are four major counties around Qinghai Lake, i.e., Tianjun, Gangcha, Gonhe, and Haiyan, with a total population of ~230,000 in 2010. Urban areas (e.g., Xining) are located ~180 km southeast of Qinghai Lake.

2.2 Sampling and analysis

An automatic precipitation sampler (SYC-2, Laoshan Electronic Instrument Complex Co., Ltd., China) was used to collect the precipitation samples (Wang et al. 2018). The sampler mainly contains three sections of a rain sensor, a rain container, and a dust preventing funnel lid. Once the rain sensor detects the precipitation, the funnel lid will be open automatically exposing the rain container to collect the rainwater. The rainwater was collected with a high-density polyethylene plastic bottle, and these bottles were pretreated using the ultra-pure water (a resistivity of 18.2 M Ω cm) until the electric conductivity (EC) was less than 2 μ s cm⁻¹. The rain sensor becomes dry after the rain, and the funnel lid will be closed to avoid the influences of dry deposition or other contaminations. The sensitivity of the rain sensor is

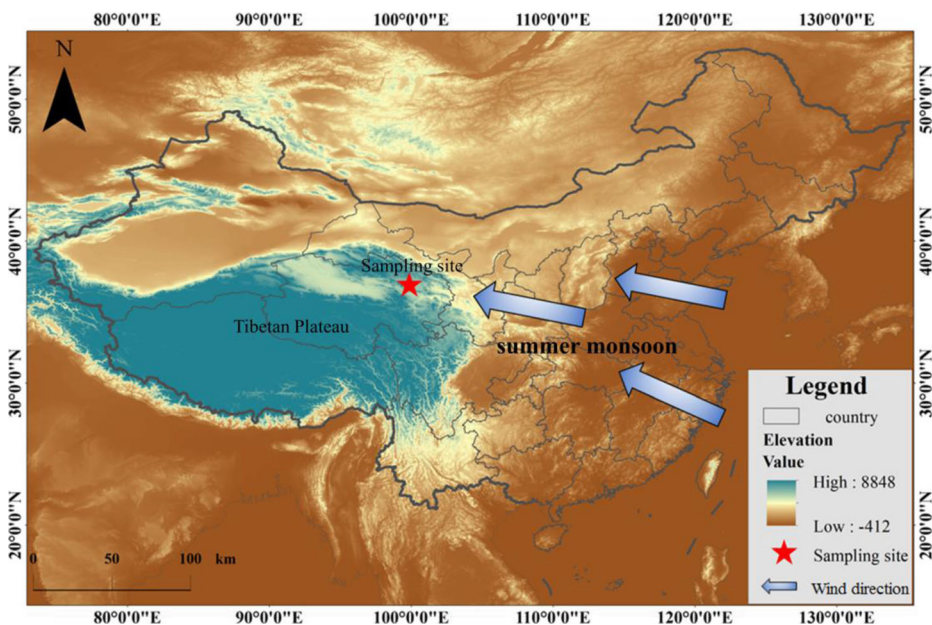


Fig. 1 Location of sampling site

$\leq 0.03 \text{ mm min}^{-1}$, and the delay time of funnel lid is $\leq 30 \text{ s}$ for opening and $\leq 5 \text{ min}$ for closing. The amount of precipitation was recorded by a rain gauge for each precipitation event. The sample collection pipeline can be automatically cleaned using the ultra-pure water before next sampling. In this study, each precipitation sample represents one rainfall event, and the collection periods last for 0.5–44 h. The insoluble particles in the rainwater were filtered with a $0.45 \mu\text{m}$ pore size microporous membrane before the samples being stored at $4 \text{ }^\circ\text{C}$ in a refrigerator. The storage time for rainwater samples was usually less than one month before the chemical analysis.

The pH and EC were measured immediately after sampling using a Mettler-Toledo Delta 320 pH meter (Mettler Corp., Greifensee, Switzerland) and a conductivity meter of DDB - 303A type (Leici Corp., Shanghai, China), respectively. The concentrations of four anions (F^- , Cl^- , NO_3^- , and SO_4^{2-}) and five cations (Na^+ , NH_4^+ , K^+ , Mg^{2+} , and Ca^{2+}) in rainwater samples were determined with a Dionex-500 ion chromatograph (IC, Dionex Corp., Sunnyvale, CA, USA). Anions were separated by an IonPac AS14A column (Dionex Corp.) with the use of $8 \text{ mM Na}_2\text{CO}_3/1 \text{ mM NaHCO}_3$ as the eluent. Cations were measured using an IonPac CS12A column (Dionex Corp.) with 20 mM methanesulfonate as the eluent. The limit of detection was less than 0.05 mg L^{-1} for each measured anion and cation. The maximum relative precisions for F^- , Cl^- , NO_3^- , SO_4^{2-} , Na^+ , NH_4^+ , K^+ , Mg^{2+} , and Ca^{2+} were 1.4%, 0.3%, 2.6%, 1.2%, 1.8%, 0.9%, 0.6%, 1.0%, and 4.0%, respectively. Standard reference materials produced by the National Research Center for Certified Reference Materials in China were analyzed for quality assurance and quality control purposes. Three field blanks were collected during the campaign, and the measured blank values were subtracted from the samples' concentrations. The repeatability of samples was found to be ranging from 0.1%–14.8% for the water-soluble ions, which were measured in the Department of Environmental Engineering, Xi'an Jiaotong University, China.

Nondispersive infrared absorption total organic carbon (TOC) analyzer (model ET1020A) was used to obtain the concentrations of dissolved organic carbon (DOC) in precipitation (Shen et al. 2014, 2017). When the pretreated rainwater sample was imported into the TOC analyzer, DOC and dissolved inorganic carbon (DIC) were both transformed into carbon dioxide (CO_2) due to the high-temperature catalytic oxidation at high-temperature combustion tube. The DIC was decomposed into CO_2 in the low-temperature reaction tube. These two kinds of CO_2 produced in the tube were imported to a nondispersive infrared inspection detector. The intensity of infrared absorption is proportional to its loading under a given wavelength, and then the concentrations of dissolved carbon (DC) and DIC can be determined. The concentration of DOC was calculated from the difference between a total carbon channel and inorganic carbon channel, that is, $\text{DOC} = \text{DC} - \text{DIC}$. DOC analysis was conducted at the Key Laboratory of Aerosol Chemistry and Physics, Institute of Earth Environment, Chinese Academy of Sciences.

Stable oxygen isotope ratio ($\delta^{18}\text{O}$) was measured at the Key Laboratory of Cryosphere and Environment, Chinese Academy of Sciences using a FinniganTM MAT-252 isotope-ratio mass spectrometer (Thermo Electron Corporation, Waltham, MA, USA). The instrument has a measurement accuracy of $\pm 0.05\text{‰}$. $^{18}\text{O}/^{16}\text{O}$ ratio ($\delta^{18}\text{O}$) was defined as the conventional δ notation in parts per thousand relatives to the Vienna standard mean ocean water.

2.3 Neutralization factor (NF) and enrichment factor (EF)

The NF was used to evaluate the neutralization of rainwater by each alkaline chemical species, and it was calculated as Eq. (1) (Bisht et al. 2017; Zhao et al. 2013):

$$NF_{X_i} = \frac{[X_i]}{[NO_3^-] + [SO_4^{2-}]} \quad (1)$$

where X_i is the chemical component of interest ion (e.g., Ca^{2+} , Mg^{2+} , NH_4^+ , Na^+ , and K^+), with all ions were expressed in $\mu\text{eq L}^{-1}$.

Furthermore, EF was used to identify the potential sources of ions. In the present study, Na^+ and Ca^{2+} were used as the reference elements for marine and crustal sources, respectively (Xiao 2016; Huang et al. 2008). EFs of the rainwater can be calculated from the following Eqs. (2) and (3):

$$EF_{marine} = \left[\frac{X}{Na^+} \right]_{rainwater} / \left[\frac{X}{Na^+} \right]_{marine} \quad (2)$$

$$EF_{crust} = \left[\frac{X}{Ca^{2+}} \right]_{rainwater} / \left[\frac{X}{Ca^{2+}} \right]_{crust} \quad (3)$$

where X is the concentration of interested ion; $[X/Na^+]_{marine}$ is the ratio from seawater composition, and $[X/Ca^{2+}]_{crust}$ represents the ratio from crustal composition. The contribution of marine component for a given ion X ($X = Cl^-$, NO_3^- , SO_4^{2-} , K^+ , Ca^{2+} , and Mg^{2+}) was further calculated using the following Eq. (4):

$$[X]_{marine} = [Na^+]_{rainwater} \times ([X]/[Na^+]_{seawater}) \quad (4)$$

3 Results and discussion

3.1 Precipitation pH and EC

The precipitation amount in this study varied from 0.5 to 39.2 mm for each event, with highest value in August (55.6 mm), followed by June (18.7 mm) and July (18.6 mm). The pH of rainwater varied from 6.1 to 8.2 with a volume-weighted mean (VWM) of 7.2 in the whole sampling period (Table 1), which was larger than the value of 5.6 in natural rainwater at equilibrium with atmospheric CO_2 . Thus, the rainwater in Qinghai Lake was considered to be alkalinized or alkaline. Figure 2 shows the pH distribution, which shows that the majority values were in the range of 6.5–7.5, amounting to approximately 63.3% of the total samples. As shown in Table 1, the largest VWM of pH was found in August with a value of 7.3, followed by 7.2 in July and 6.7 in June. Alkaline rainwater also has been found in other studies on the Tibetan Plateau. For example, Li et al. (2007) reported that the precipitation pH values varied from 6.0 to 7.4 with an average of 6.6 at Nam Co; Yang et al. (2012) found that the rainwater had an average pH of 7.9 in the Shigatse region; and Zhang et al. (2012b) indicated that the average pH value was 6.1 at Lijiang.

Table 1 Volume-weighted mean (VWM) concentrations of major ions ($\mu\text{eq L}^{-1}$), pH values, and electric conductivity (EC, $\mu\text{s cm}^{-1}$), dissolved organic carbon (DOC, $\mu\text{eq L}^{-1}$), $\delta^{18}\text{O}$ (‰) in rainwater during the campaign

Month		pH	EC	DOC	$\delta^{18}\text{O}$	Na^+	NH_4^+	K^+	Mg^{2+}	Ca^{2+}	F^-	Cl^-	NO_3^-	SO_4^{2-}
June	Max	8.03	70.30	10.84	-3.85	64.07	138.48	38.52	66.38	231.34	3.58	23.60	66.33	151.49
	Min	6.05	7.82	0.55	-11.49	7.99	20.11	1.20	3.77	1.61	0.90	8.37	4.90	19.25
	VWM	6.67	21.44	1.94	-5.85	25.09	56.92	3.58	8.62	56.95	1.21	17.26	19.88	58.94
July	Max	8.19	26.40	6.91	-5.19	38.37	52.89	14.30	30.34	83.57	7.59	32.73	29.98	58.23
	Min	6.60	6.02	0.96	-8.26	11.25	6.88	1.49	5.58	25.35	3.08	12.77	6.78	7.53
	VWM	7.22	18.17	1.90	-5.00	16.83	23.94	4.30	12.71	53.67	4.39	18.61	13.98	26.14
August	Max	7.88	320.00	8.35	-6.12	44.35	49.80	68.61	675.86	662.92	17.99	43.81	111.20	810.90
	Min	6.96	7.92	0.65	-13.50	5.33	4.81	1.14	4.73	11.13	3.18	8.45	1.46	5.30
	VWM	7.31	18.50	1.06	-9.77	15.53	23.85	3.67	22.08	157.44	4.10	22.47	9.47	26.35
Total	VWM	7.17	19.01	1.40	-8.05	17.66	30.35	3.78	17.56	116.94	3.59	20.67	12.41	32.69

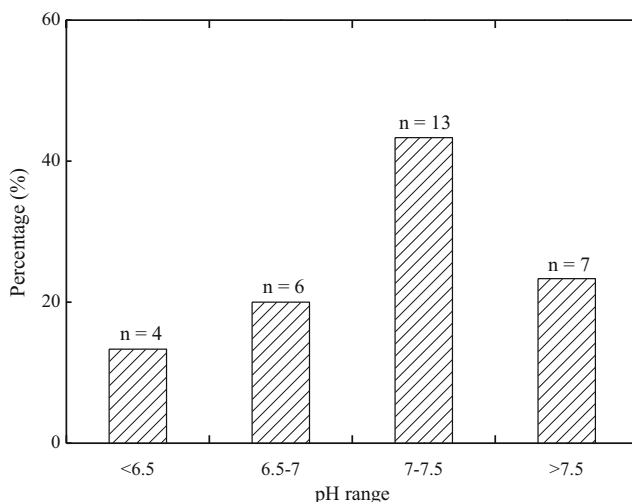


Fig. 2 Frequency distribution of pH values of all precipitation events

Ca^{2+} and Mg^{2+} exhibited exponential increase with pH, and together accounted for 43.4%, 32.2%, 43.6%, and 46.0% of the total measured ions at pH of <6.5, 6.5–7.0, 7.0–7.5, and >7.5, respectively. Meanwhile, the ions of SO_4^{2-} and NO_3^- together amounted to 21.4%, 29.1%, 19.1%, and 33.7% at pH of <6.5, 6.5–7.0, 7.0–7.5, and >7.5, respectively. As the major alkaline ion, the concentration of Ca^{2+} was enhanced at larger pH, which was consistent with the greater abundances of alkaline materials in the rainwater. Meanwhile, Ca^{2+} correlated well with SO_4^{2-} ($r=0.88$), suggesting that those acidic materials can be adsorbed to particulate matter and be neutralized by Ca^{2+} in the particles. Indeed, the total suspended particulate collected in Qinghai Lake is known to be rich in Ca^{2+} (Zhang et al. 2014a). Moreover, Zhang et al. (2003) monitored the pH in Qinghai Lake during 1980–1990, and found that precipitation exhibited alkaline, which was caused by airborne dusts from local alkaline soils.

As shown in Table 1, the precipitation EC ranged from 6.0 to 320.0 $\mu\text{s cm}^{-1}$, with a VWM of 19.0 $\mu\text{s cm}^{-1}$. The EC value was higher in June with a VWM of 21.4 $\mu\text{s cm}^{-1}$ compared with those in August (18.5 $\mu\text{s cm}^{-1}$) and July (18.2 $\mu\text{s cm}^{-1}$). The precipitation EC can be used to indicate the level of total soluble ionic components to some extent (Gioda et al. 2013). Higher VWM of EC (21.4 $\mu\text{s cm}^{-1}$) was observed in June reflecting the worse atmospheric environmental quality and anthropogenic pollution, e.g., enhanced tourism, which increased more motor vehicles and catering industry with use of biofuels and coal. The increased anthropogenic activities emitted a large number of pollutants into atmosphere. This phenomenon was consistent with the larger loadings of atmospheric TSP in this month (Zhang et al. 2014a). Compared with other studies on Tibetan Plateau and its surrounding areas, the average EC during June to August in Qinghai Lake was comparable with those observed in the Shigatse region (21.6 $\mu\text{s cm}^{-1}$, Yang et al. 2012) and Nam Co (19.7 $\mu\text{s cm}^{-1}$, Li et al. 2007). However, the EC in Qinghai Lake was lower than those of urban or remote towns of Tibet, such as Lhasa (25.6 $\mu\text{s cm}^{-1}$), Amdo (28.4 $\mu\text{s cm}^{-1}$), and Dingri (29.1 $\mu\text{s cm}^{-1}$) (Zhang et al. 2003).

3.2 Chemical composition and acid neutralization

The concentrations of water-soluble ions in the rainwater samples are summarized in Table 1. The total ionic concentrations varied widely by 35-fold from 69.5 to 2423.2 $\mu\text{eq L}^{-1}$ with a VWM of 255.7 $\mu\text{eq L}^{-1}$ during the entire campaign. The VWM values for total anions and cations were 69.4 and 186.3 $\mu\text{eq L}^{-1}$, respectively. The total anions were the highest in June, followed by July and August. In contrast, the total cations were the highest in August, followed by June and July. It should be noted that a sample collected on 17 August had high total anions (966.0 $\mu\text{eq L}^{-1}$) and cations (1457.2 $\mu\text{eq L}^{-1}$), which were 26 and 54 times higher than the lowest values during the campaign. The large obtained values may be due to the effectively removed particulate matter from the atmosphere. The total anions correlated significantly with the total cations ($r = 0.97$, $p < 0.01$) with a slope ($\Sigma\text{anions}/\Sigma\text{cations}$) of 0.64 (Fig. 3), indicating that some anions were missed. The anions deficiency here may be due to the lack of measurements of $\text{HCO}_3^-/\text{CO}_3^{2-}$ and organic acids (Jinfu et al. 2011; Meng et al. 2013). This phenomenon was also observed in the rainwater samples collected in other sites on the Tibetan Plateau (Li et al. 2007; Yang et al. 2012).

As shown in Table 1, the ionic abundance followed the sequence of $\text{SO}_4^{2-} > \text{Cl}^- > \text{NO}_3^- > \text{F}^-$ for anions and $\text{Ca}^{2+} > \text{NH}_4^+ > \text{Na}^+ > \text{Mg}^{2+} > \text{K}^+$ for cations. Among these ions, Ca^{2+} was the most abundant species, accounting for 45.7% of the total measured ions and 62.8% of the total cations. The high contribution of Ca^{2+} can be explained by the influence of the continental dust rich in calcium (Jinfu et al. 2011). However, the concentrations of Ca^{2+} varied largely from 1.6 to 662.9 $\mu\text{eq L}^{-1}$ with the various individual precipitation events. The highest monthly average concentration of Ca^{2+} was found in August (157.4 $\mu\text{eq L}^{-1}$), followed by June (57.0 $\mu\text{eq L}^{-1}$) and July (53.7 $\mu\text{eq L}^{-1}$). Ca^{2+} in continental dust usually exists in coarse mode, and thus higher precipitation amount in August compared with other months favors Ca^{2+} scavenging out of the atmosphere. SO_4^{2-} was the second most abundant ion, which amounted to 12.8% of the total ions and 47.1% of the total anions. SO_4^{2-} is formed from precursor gas of SO_2 through heterogeneous reactions (Wang et al. 2016), and its relative high concentration may reflect the influence of anthropogenic activities (e.g., coal burning) from surrounding areas.

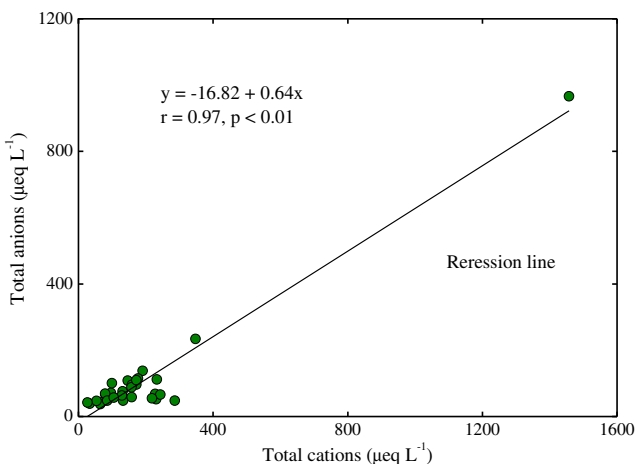


Fig. 3 Scatter plot of total anions versus total cations

Previous studies have indicated that the main acidifying composition in rainwater samples are mainly H_2SO_4 and HNO_3 , while crustal materials (e.g., Ca^{2+} and Mg^{2+}) are the main acid-neutralizing components (Pu et al. 2017; Zhang et al. 2012c). To evaluate the neutralization of rainwater by each alkaline chemical species, NFs were calculated based on the Eq. (1). In this study, the NF values for Ca^{2+} , Mg^{2+} , NH_4^+ , Na^+ , and K^+ in rainwater were estimated to be 1.11, 0.47, 0.41, 0.28, and 0.09, respectively, indicating that Ca^{2+} and Mg^{2+} were the dominant neutralization substances, whereas the neutralization by Na^+ and K^+ can be negligible.

DOC is a ubiquitous and key component in atmospheric water. One of the most significant aspects of DOC geochemistry in the troposphere is its role in the removal of incompletely oxidized carbon from the atmosphere via wet deposition (Willey et al. 2000). Rainwater DOC is a major component of the dissolved material in rain in many regions of the world, and it includes both biogenic and anthropogenic carbon (Li et al. 2018; Andreae et al. 1990; Fraser et al. 1998). The concentrations of DOC in the rainwater samples in Qinghai Lake spanned two orders of magnitude, from 0.6 to 10.8 mg L^{-1} with a VWM value of 1.4 mg L^{-1} (Table 1), and the highest value was found in June (1.94 mg L^{-1}), followed by July (1.90 mg L^{-1}) and August (1.06 mg L^{-1}). The average DOC in this study was higher than several sites on the Tibetan Plateau, such as Lhasa (1.1 mg L^{-1}), Nam Co (1.1 mg L^{-1}), Lulang (0.8 mg L^{-1}), and Everest (0.9 mg L^{-1}) (Li et al. 2016, 2017a). The large variations of DOC concentrations in this study could be attributed to the differences in the sources of OC. For example, our sampling site is strongly influenced by anthropogenic activities from inland China, leading to impact from various sources of OC. Furthermore, the concentration of DOC was associated with the rainfall amount. The DOC concentration shows a roughly negative power function with the precipitation amount ($r = -0.48$), suggesting that the DOC tends to be effectively scavenging from the atmosphere within the initial period of the rainfall event. Similar relationship between DOC concentration and precipitation amount also has been found in other studies (Pan et al. 2010; Balla et al. 2014).

The $\delta^{18}\text{O}$ in the rainwater in Qinghai Lake varied from -13.5‰ to -3.9‰ with an average of -8.1‰ during the whole sampling period (Table 1). The highest $\delta^{18}\text{O}$ was observed in July (-5.0‰), followed by June (-5.85‰) and August (-9.77‰). This value was comparable with those in Delingha, northern Tibetan Plateau (-7.0‰ in the period of February – September, 2007, Yang and Yao 2016) and Yushu, central Tibetan Plateau (-8.3‰ in the period of January – December, 2007, Yang and Yao 2016), but higher than those in Lulang, southeastern Tibetan Plateau (-13.8‰ in the period of January – November, 2007, Yang and Yao 2016), Deqin, southeastern margin of the Tibetan Plateau (-13.2‰ in the period of June – September, 2012, Yu et al. 2016), and Yushu, eastern Tibetan Plateau (-13.8‰ in the period of July – September, 2001–2002, Tian et al. 2008). Compared with the values in glaciers, $\delta^{18}\text{O}$ in this study was similar to that in Shiyi Glacier, north of Tibetan Plateau (-8.3‰ , Zongxing in the period of July 2012 – November 2013, et al., 2015), but higher than that in Baishui Glacier, southeastern Tibetan Plateau (-10.7‰ , Pang et al. 2012). Previous studies have indicated that the values of $\delta^{18}\text{O}$ can be affected by the precipitation amount and temperature effect, these are, “amount effect” and “temperature effect”. For example, by analyzing isotopic composition in precipitation in Lijiang, Zhang et al. (2014b) and Pang et al. (2006) both indicated that “amount effect” was the main factor influencing $\delta^{18}\text{O}$ variations for each precipitation event, while the “temperature effect” could be ignored. Moreover, the “amount effect” in $\delta^{18}\text{O}$ was also found on the South Tibetan Plateau (Tian et al. 2008), which was affected by the southwest monsoon. However, in this study, there was no significant correlation between $\delta^{18}\text{O}$ and precipitation amount, which indicates that there was other factor influencing $\delta^{18}\text{O}$ in our rainwater samples.

3.3 Origins of major ions in the rainwater

The EF is a useful method to identify the potential sources of ions, and it is calculated by comparing the ratio found between ions collected in rainwater to the corresponding ionic ratio presented in the Earth's crust or seawater based on the Eqs. (2) and (3). As shown in Table 2, the mean value of Cl^-/Na^+ in the rainwater was 0.96, which was close to the seawater ratio of 1.17. Thus, the Na^+ and Cl^- in the rainwater should mainly from marine origin. In addition, the vapor evaporated from Qinghai Lake may also influence the precipitation in some extent. For example, Cui and Li (2015) reported that the annual contribution of lake evaporation to basin precipitation was 23.4%. The ratio of $\text{NO}_3^-/\text{Na}^+$ in the rainwater was 0.48 with the EF of 24,026, indicating negligible contribution from marine to NO_3^- . Moreover, the marine contribution to K^+ was also negligible. Local biogenic sources come from regional activities such as yak dung combustion for heating and cooking and the excretion of yaks and horse could account for the highly enrichments of K^+ and NO_3^- in precipitation in the Lake Qinghai area.

To further estimate the contribution of each source to ions in precipitation, Na^+ was assumed to be of marine origin while F^- , Cl^- , NO_3^- , and NH_4^+ were assumed to have an ignored crustal source. The proportions of sea salt and terrestrial end-members were therefore calculated based on Eq. (4). The ratios of X/Na^+ were determined according to the composition of seawater. If Mg^{2+} was assumed to be composed of marine and crustal sources only, the crustal part of Ca^{2+} and K^+ could be calculated by the equivalent $[\text{Ca}^{2+}/\text{Mg}^{2+}]_{\text{crustal}}$ and $[\text{K}^+/\text{Mg}^{2+}]_{\text{crustal}}$ ratios of 1.87 and 0.48, respectively. Assuming SO_4^{2-} from the crustal source was supplied by gypsum, it could be calculated using the formula $[\text{SO}_4^{2-}]_{\text{crustal}} = 0.47[\text{Ca}^{2+}]_{\text{crustal}}$, so the anthropogenic SO_4^{2-} could be calculated using the following formula: $[\text{SO}_4^{2-}]_{\text{anthropogenic}} = [\text{SO}_4^{2-}]_{\text{total}} - [\text{SO}_4^{2-}]_{\text{marine}} - [\text{SO}_4^{2-}]_{\text{crustal}}$. Table 3 shows the estimated contributions from different sources to the chemical composition of precipitation. Of all these species, SO_4^{2-} , NH_4^+ , and NO_3^- were dominated by the anthropogenic source. SO_4^{2-} in rainwater may also originate from anthropogenic emissions of SO_2 . The Qinghai Lake area has almost no industrial emissions, and the local residents only use dung (the excretion of yaks and horses) for heating and cooking. The proportion of SO_4^{2-} concentrated in anthropogenic (85.8%) and it can also be found in the proportion of NO_3^- (100%). Furthermore, a highly positive correlation between SO_4^{2-} and NO_3^- ($r = 0.90$) was observed, indicating that they were from similar sources, which may reflect the input of pollutants from dung combustion in Qinghai Lake area. The proportion of Cl^- coming from marine was about 100%. The marine input of Cl^- could come from evaporative ions of Qinghai Lake which can also be found in the $\text{EF}_{\text{marine}}$ of Cl^- ($\text{EF} = 0.82$).

Table 2 Enrichment factors (EFs) for rainwater components in Qinghai Lake relative to the crust and seawater

	$\text{SO}_4^{2-}/\text{Na}^+$	$\text{NO}_3^-/\text{Na}^+$	Cl^-/Na^+	$\text{Ca}^{2+}/\text{Na}^+$	$\text{Mg}^{2+}/\text{Na}^+$	K^+/Na^+
Seawater ^a	0.12	0.00002	1.17	0.044	0.23	0.022
rainwater	1.36	0.48	0.96	4.63	0.75	0.12
$\text{EF}_{\text{marine}}$	11.34	24,026	0.82	105	3.26	7.09
	$\text{SO}_4^{2-}/\text{Ca}^{2+}$	$\text{NO}_3^-/\text{Ca}^{2+}$	$\text{Cl}^-/\text{Ca}^{2+}$	$\text{Na}^+/\text{Ca}^{2+}$	$\text{Mg}^{2+}/\text{Ca}^{2+}$	$\text{K}^+/\text{Ca}^{2+}$
Soil	0.045	0.0065	0.0055	0.65	0.34	0.99
rainwater	0.43	0.16	0.26	0.29	0.18	0.047
EF_{crust}	9.58	24.77	47.45	0.44	0.52	0.048

^a the ratios of ions to Na^+ were cited from Keene et al. (1986)

Table 3 Proportions (%) of the source contributions in the rainwater samples

	Marine (%)	Crustal (%)	Anthropogenic (%)
F ⁻	0.00	0.00	100
SO ₄ ²⁻	8.82	5.42	85.76
NO ₃ ⁻	0.00	0.00	100
Cl ⁻	100	0.00	0.00
Ca ²⁺	0.95	32.75	66.30
Mg ²⁺	30.72	69.28	0.00
K ⁺	14.11	18.05	69.84
NH ₄ ⁺	0.00	0.00	100

The Ca²⁺ in the rainwater from the Qinghai Lake area was likely crustal origin and anthropogenic, coming from soil dust suspended in the lower troposphere (Ali et al. 2004; Wang and Han 2011). According to Flues et al. (2002), high concentrations of rainwater NH₄⁺ could be related to gaseous ammonia (NH₃) introduced into the atmosphere, mainly by cattle breeding (80%), fertilizer use (17%), and industrial processes. Agriculture activities exhaust enormous NH₃ to the atmosphere in the Qinghai Lake area coinciding with the fact of the high level of NH₄⁺ in the rainwater. Thus, it can be attributed to the presence of NH₄⁺ in the samples to a direct input of gaseous NH₃ as well as to the input of absorbed NH₄⁺ from aerosols.

3.4 Transport pathways of precipitation

Cluster analysis of air-mass trajectories was applied to characterize the transport patterns of water vapor to Qinghai Lake. This procedure combines hourly air-mass trajectories into representative spatial groups using angle-based distance statistics (Sirois and Bottenheim 1995). The three-day backward trajectories were calculated hourly for each rainfall event using the NOAA Air Resource Lab (ARL) Hybrid Single-Particle Lagrangian Integrated Trajectory (HYSPLIT) model (<https://ready.arl.noaa.gov/HYSPLIT.php>). Each arrival height of the trajectory was set to be 1500 m, and the gridded meteorological data (Global Data Assimilation System, GDAS1) were used in the HYSPLIT model. As shown in Fig. 4, about 17.5% of total backward trajectories (228) were classified as Cluster #1, and those air masses were originated from Inner Mongolia and then moved across the middle of Gansu province. Cluster #2 originated from northeastern edge of Sinkiang province, and the air passed through northwest of Gansu province. This cluster accounted for 10.2% of total trajectories. The trajectories in Cluster #3 contributed to 61.8% of total numbers, and this Cluster was derived from south of Gansu province and then went through the east of Qinghai province. The air masses associated with Cluster #4 passed over the west of Qinghai province (Tsaidam Basin) and accounted for 10.5% of total trajectories.

As shown in Table 4, the values of $\delta^{18}\text{O}$ were lower for Cluster #4 (-8.9‰) and Cluster #1 (-7.0‰) compared with Cluster #3 (-4.8‰) and Cluster #2 (-3.8‰). The VWM value for total cations was highest for Cluster #4 ($194.8 \mu\text{eq L}^{-1}$), followed by Cluster #1 ($164.7 \mu\text{eq L}^{-1}$), Cluster #3 ($142.4 \mu\text{eq L}^{-1}$), and Cluster #2 ($131.8 \mu\text{eq L}^{-1}$). In contrast, the VWM value for total anions was largest for Cluster #1 ($105.2 \mu\text{eq L}^{-1}$), followed by Cluster #3 ($74.1 \mu\text{eq L}^{-1}$), Cluster #4 ($57.7 \mu\text{eq L}^{-1}$), and Cluster #2 ($55.0 \mu\text{eq L}^{-1}$). Among those water-soluble inorganic ions, higher VWM values of NH₄⁺, SO₄²⁻, and NO₃⁻ were observed for Cluster #1 and #3 compared with Cluster #2 and #4. This can be explained by the more anthropogenic

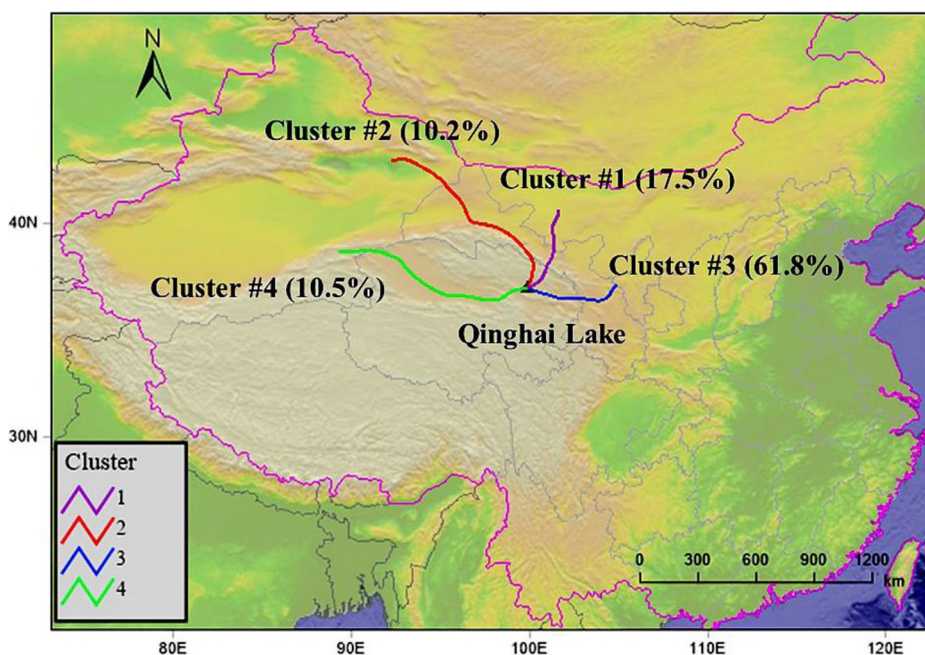


Fig. 4 Mean trajectory clusters map for the rainfall events

activities due to more industrialization and urbanization areas in the middle and south of Gansu province. The VWM value for Ca^{2+} was the largest for Cluster 4#, and this was associated with the air masses passed through the Tsaidam Basin with the high loading of Ca^{2+} .

4 Conclusions

A study was conducted on chemical compositions (ions, DOC, and oxygen isotopic composition) and sources of rainwater in a remote area of Qinghai Lake, northeastern Tibetan Plateau, from June to August 2010. The total ionic concentrations varied widely by 35-fold from 69.5 to 2423.2 $\mu\text{eq L}^{-1}$ with a VWM of 255.7 $\mu\text{eq L}^{-1}$ during the entire campaign. Ca^{2+} was the most abundant species, accounting for 45.7% of the total ion mass and 62.8% of the total cation mass. Moreover, Ca^{2+} was also the dominant neutralization substance, which exhibited exponential increase with pH, consistent with the greater abundances of alkaline materials in the rainwater. Meanwhile, Ca^{2+} correlated well with SO_4^{2-} , suggesting that those acidic materials can be adsorbed to particulate matter and be neutralized by Ca^{2+} in the particles.

Table 4 Volume-weighted mean (VWM) concentrations of major ions ($\mu\text{eq L}^{-1}$) and $\delta^{18}\text{O}$ (‰) in the rainwater for each cluster

Type	Na^+	NH_4^+	K^+	Mg^{2+}	Ca^{2+}	F^-	Cl^-	NO_3^-	SO_4^{2-}	$\delta^{18}\text{O}$
Cluster #1	32.24	43.32	5.00	15.22	68.94	3.27	29.86	21.56	50.49	-7.01
Cluster #2	32.76	19.81	9.95	15.10	54.14	2.14	16.48	9.46	26.93	-3.83
Cluster #3	13.76	29.89	3.79	13.73	81.24	6.04	16.87	17.88	33.36	-4.82
Cluster #4	14.30	27.53	3.10	16.64	133.24	3.34	19.07	9.27	26.05	-8.86

The average concentration of DOC in the rainwater samples in Qinghai Lake was 1.4 mg L^{-1} . The DOC concentration showed a roughly negative power function with the precipitation amount, suggesting that the DOC tends to be effectively scavenging from the atmosphere within the initial period of the rainfall event. The values of $\delta^{18}\text{O}$ in the rainwater in Qinghai Lake averaged -8.1‰ and shows no significant correlation with precipitation amount, which indicates that there may be other factor influencing $\delta^{18}\text{O}$ in our rainwater samples. The EF analysis indicates that crustal materials from continental dust were the major sources for these ions. The air masses associated with northeast and east had high VWM values of NH_4^+ , SO_4^{2-} , and NO_3^- , whereas high Ca^{2+} loading was related to the air mass from west.

Acknowledgements This study is supported by a grant from the State Key Laboratory of Loess and Quaternary Geology, Chinese Academy of Sciences (SKLLQG1616).

References

- Ali, K., Momin, G.A., Tiwari, S., Safai, P.D., Chate, D.M., Rao, P.S.P.: Fog and precipitation chemistry at Delhi, North India. *Atmos. Environ.* **38**, 4215–4222 (2004)
- An, Z.S., Colman, S.M., Zhou, W.J., Li, X.Q., Brown, E.T., Jull, A.J.T., Cai, Y.J., Huang, Y.S., Lu, X.F., Chang, H., Song, Y.G., Sun, Y.B., Xu, H., Liu, W.G., Jin, Z.D., Liu, X.D., Cheng, P., Liu, Y., Ai, L., Li, X.Z., Liu, X.J., Yan, L.B., Shi, Z.G., Wang, X.L., Wu, F., Qiang, X.K., Dong, J.B., Lu, F.Y., Xu, X.W.: Interplay between the westerlies and Asian monsoon recorded in Lake Qinghai sediments since 32 ka. *Sci. Rep.* **2**, 619 (2012). <https://doi.org/10.1038/srep00619>
- Andreae, M., Talbot, R., Berresheim, H., Beecher, K.: Precipitation chemistry in Central Amazonia. *J. Geophys. Res.: Atmos.* **95**, 16987–16999 (1990)
- Balla, D., Papageorgiou, A., Voutsas, D.: Carbonyl compounds and dissolved organic carbon in rainwater of an urban atmosphere. *Environ. Sci. Pollut. Res.* **21**, 12062–12073 (2014)
- Bisht, D.S., Srivastava, A.K., Joshi, H., Ram, K., Singh, N., Naja, M., Srivastava, M.K., Tiwari, S.: Chemical characterization of rainwater at a high-altitude site “Nainital” in the Central Himalayas, India. *Environ. Sci. Pollut. Res.* **24**, 3959–3969 (2017)
- Cangemi, M., Madonia, P., Favara, R.: Chemical characterisation of rainwater at Stromboli Island (Italy): the effect of post-depositional processes. *J. Volcanol. Geotherm. Res.* **335**, 82–91 (2017)
- Cui, B.-L., Li, X.-Y.: Stable isotopes reveal sources of precipitation in the Qinghai Lake Basin of the northeastern Tibetan plateau. *Sci. Total Environ.* **527–528**, 26–37 (2015)
- Flues, M., Hama, P., Lemes, M.J.L., Dantas, E.S.K., Fornaro, A.: Evaluation of the rainwater acidity of a rural region due to a coal-fired power plant in Brazil. *Atmos. Environ.* **36**, 2397–2404 (2002)
- Fraser, M.P., Cass, G.R., Simoneit, B.R.T.: Gas-phase and particle-phase organic compounds emitted from motor vehicle traffic in a Los Angeles roadway tunnel. *Environ. Sci. Technol.* **32**, 2051–2060 (1998)
- Gioda, A., Mayol-Bracero, O.L., Scatena, F.N., Weathers, K.C., Mateus, V.L., McDowell, W.H.: Chemical constituents in clouds and rainwater in the Puerto Rican rainforest: potential sources and seasonal drivers. *Atmos. Environ.* **68**, 208–220 (2013)
- Huang, Y., Wang, Y., Zhang, L.: Long-term trend of chemical composition of wet atmospheric precipitation during 1986–2006 at Shenzhen City, China. *Atmos. Environ.* **42**, 3740–3750 (2008)
- JinFu, Z., Kelong, C., Shengkui, C., Liang, C., Yanpeng, W., Baoliang, L., Yongsheng, W.: Spatial variability analysis of soil salt and its component ions in Qinghai Lake region. *Procedia Environ. Sci.* **10**, 2431–2436 (2011)
- Kang, S.C., Xu, Y.W., You, Q.L., Flugel, W.A., Pepin, N., Yao, T.D.: Review of climate and cryospheric change in the Tibetan plateau. *Environ. Res. Lett.* **5**, 015101 (2010)
- Keene, W.C., Pszenny, A.A.P., Galloway, J.N., Hawley, M.E.: Sea-salt corrections and interpretation of constituent ratios in marine precipitation. *J. Geophys. Res.: Atmos.* **91**, 6647–6658 (1986)
- Li, C., Kang, S., Zhang, Q., Kaspari, S.: Major ionic composition of precipitation in the Nam co region, central Tibetan plateau. *Atmos. Res.* **85**, 351–360 (2007)
- Li, C., Yan, F., Kang, S., Chen, P., Qu, B., Hu, Z., Sillanpää, M.: Concentration, sources, and flux of dissolved organic carbon of precipitation at Lhasa city, the Tibetan plateau. *Environ. Sci. Pollut. Res.* **23**, 12915–12921 (2016)

- Li, C., Yan, F., Kang, S., Chen, P., Hu, Z., Han, X., Zhang, G., Gao, S., Qu, B., Sillanpää, M.: Deposition and light absorption characteristics of precipitation dissolved organic carbon (DOC) at three remote stations in the Himalayas and Tibetan Plateau, China. *Sci. Total Environ.* **605–606**, 1039–1046 (2017a)
- Li, X.F., Kang, S.C., He, X.B., Qu, B., Tripathee, L., Jing, Z.F., Paudyal, R., Li, Y., Zhang, Y.L., Yan, F.P., Li, G., Li, C.L.: Light-absorbing impurities accelerate glacier melt in the central Tibetan Plateau. *Sci. Total Environ.* **587**, 482–490 (2017b)
- Li, C., Chen, P., Kang, S., Yan, F., Tripathee, L., Wu, G., Qu, B., Sillanpää, M., Yang, D., Dittmar, T., Stubbins, A., Raymond Peter, A.: Fossil fuel combustion emission from South Asia influences precipitation dissolved organic carbon reaching the remote Tibetan plateau: isotopic and molecular evidence. *J. Geophys. Res.: Atmos.* **123**, 6248–6258 (2018)
- Meng, J., Wang, G., Li, J., Cheng, C., Cao, J.: Atmospheric oxalic acid and related secondary organic aerosols in Qinghai Lake, a continental background site in Tibet Plateau. *Atmos. Environ.* **79**, 582–589 (2013)
- Nadzir, M.S.M., Lin, C.Y., Khan, M.F., Latif, M.T., Dominick, D., Hamid, H.H.A., Mohamad, N., Maulud, K.N.A., Wahab, M.I.A., Kamaludin, N.F., Lazim, M.A.S.M.: Characterization of rainwater chemical composition after a Southeast Asia haze event: insight of transboundary pollutant transport during the northeast monsoon. *Environ. Sci. Pollut. Res.* **24**, 15278–15290 (2017)
- Pan, Y., Wang, Y., Xin, J., Tang, G., Song, T., Wang, Y., Li, X., Wu, F.: Study on dissolved organic carbon in precipitation in northern China. *Atmos. Environ.* **44**, 2350–2357 (2010)
- Pang, H., He, Y., Lu, A., Zhao, J., Ning, B., Yuan, L., Song, B.: Synoptic-scale variation of $\delta^{18}\text{O}$ in summer monsoon rainfall at Lijiang, China. *Chin. Sci. Bull.* **51**, 2897–2904 (2006)
- Pang, H., He, Y., Hou, S., Zhang, N.: Changes in ionic and oxygen isotopic composition of the snow-firn pack at Baishui glacier no. 1, southeastern Tibetan plateau. *Environ. Earth Sci.* **67**, 2345–2358 (2012)
- Pu, W., Quan, W., Ma, Z., Shi, X., Zhao, X., Zhang, L., Wang, Z., Wang, W.: Long-term trend of chemical composition of atmospheric precipitation at a regional background station in northern China. *Sci. Total Environ.* **580**, 1340–1350 (2017)
- Qian, Y., Yasunari, T.J., Doherty, S.J., Flanner, M.G., Lau, W.K.M., Ming, J., Wang, H.L., Wang, M., Warren, S.G., Zhang, R.D.: Light-absorbing particles in snow and ice: measurement and modeling of climatic and hydrological impact. *Adv. Atmos. Sci.* **32**, 64–91 (2015)
- Rao, P.S.P., Tiwari, S., Matwale, J.L., Pervez, S., Tunved, P., Safai, P.D., Srivastava, A.K., Bisht, D.S., Singh, S., Hopke, P.K.: Sources of chemical species in rainwater during monsoon and non-monsoonal periods over two mega cities in India and dominant source region of secondary aerosols. *Atmos. Environ.* **146**, 90–99 (2016)
- Seinfeld, J.H., Pandis, S.N.: *Atmospheric chemistry and physics: from air pollution to climate change*. Wiley Publishers, New York (2016)
- Shen, Z., Cao, J., Arimoto, R., Han, Z., Zhang, R., Han, Y., Liu, S., Okuda, T., Nakao, S., Tanaka, S.: Ionic composition of TSP and PM_{2.5} during dust storms and air pollution episodes at Xi'an, China. *Atmos. Environ.* **43**, 2911–2918 (2009)
- Shen, Z., Zhang, L., Cao, J., Tian, J., Liu, L., Wang, G., Zhao, Z., Wang, X., Zhang, R., Liu, S.: Chemical composition, sources, and deposition fluxes of water-soluble inorganic ions obtained from precipitation chemistry measurements collected at an urban site in Northwest China. *J. Environ. Monit.* **14**, 3000–3008 (2012)
- Shen, Z., Cao, J., Zhang, L., Liu, L., Zhang, Q., Li, J., Han, Y., Zhu, C., Zhao, Z., Liu, S.: Day–night differences and seasonal variations of chemical species in PM₁₀ over Xi'an, Northwest China. *Environ. Sci. Pollut. Res.* **21**, 3697–3705 (2014)
- Shen, Z., Zhang, Q., Cao, J., Zhang, L., Lei, Y., Huang, Y., Huang, R.J., Gao, J., Zhao, Z., Zhu, C., Yin, X., Zheng, C., Xu, H., Liu, S.: Optical properties and possible sources of brown carbon in PM_{2.5} over Xi'an, China. *Atmos. Environ.* **150**, 322–330 (2017)
- Sirois, A., Bottenheim, J.W.: Use of backward trajectories to interpret the 5-year record of PAN and O₃ ambient air concentrations at Kejimikujik National Park, Nova Scotia. *J. Geophys. Res.* **100**, 2867–2881 (1995)
- Tang, M.: Formation, evolution and variability characteristics of Qinghai-Tibetan plateau monsoon, contemporary climatic variations over Qinghai-Tibetan plateau and their influences on environments (ed. Tang, M., Chen, G., Lin, Z.), Guangdong Sci. Technology Press, Guangzhou. 161–182 (1998)
- Tian, L., Ma, L., Yu, W., Liu, Z., Yin, C., Zhao, Z., Tang, W., Wang, Y.: Seasonal variations of stable isotope in precipitation and moisture transport at Yushu, eastern Tibetan plateau. *Sci. China, Ser. D Earth Sci.* **51**, 1121–1128 (2008)
- Wang, H., Han, G.: Chemical composition of rainwater and anthropogenic influences in Chengdu, Southwest China. *Atmos. Res.* **99**, 190–196 (2011)
- Wang, Q., Schwarz, J., Cao, J., Gao, R., Fahey, D., Hu, T., Huang, R.J., Han, Y., Shen, Z.: Black carbon aerosol characterization in a remote area of Qinghai-Tibetan plateau, western China. *Sci. Total Environ.* **479**, 151–158 (2014)

- Wang, P., Cao, J., Han, Y., Jin, Z., Wu, F., Zhang, F.: Elemental distribution in the topsoil of the Lake Qinghai catchment, NE Tibetan plateau, and the implications for weathering in semi-arid areas. *J. Geochem. Explor.* **152**, 1–9 (2015)
- Wang, G., Zhang, R., Gomez, M.E., Yang, L., Levy Zamora, M., Hu, M., Lin, Y., Peng, J., Guo, S., Meng, J., Li, J., Cheng, C., Hu, T., Ren, Y., Wang, Y., Gao, J., Cao, J., An, Z., Zhou, W., Li, G., Wang, J., Tian, P., Marrero-Ortiz, W., Secrest, J., Du, Z., Zheng, J., Shang, D., Zeng, L., Shao, M., Wang, W., Huang, Y., Wang, Y., Zhu, Y., Li, Y., Hu, J., Pan, B., Cai, L., Cheng, Y., Ji, Y., Zhang, F., Rosenfeld, D., Liss, P.S., Duce, R.A., Kolb, C.E., Molina, M.J.: Persistent sulfate formation from London fog to Chinese haze. *P. Natl. Acad. Sci.* **113**, 13630 (2016)
- Wang, L., Shen, Z., Lu, D., Zhang, Q., Zhang, T., Lei, Y., Xu, H.: Water-soluble components in rainwater over Xi'an in Northwest China: source apportionment and pollution controls effectiveness evaluation. *Atmos. Pollut. Res.* **10**, 395–403 (2019)
- Willey, J.D., Kieber, R.J., Eymann, M.S., Avery, G.B.: Rainwater dissolved organic carbon: concentrations and global flux. *Global Biogeochem. Cycles.* **14**, 139–148 (2000)
- Wright, L.P., Zhang, L., Cheng, I., Aherne, J., Wentworth, G.R.: Impacts and effects indicators of atmospheric deposition of major pollutants to various ecosystems - a review. *Aerosol Air Qual. Res.* **18**, 1953–1992 (2018)
- Xiao, J.: Chemical composition and source identification of rainwater constituents at an urban site in Xi'an. *Environ. Earth Sci.* **75**, 209 (2016)
- Xiao, H.W., Xiao, H.Y., Long, A.M., Wang, Y.L., Liu, C.Q.: Chemical composition and source apportionment of rainwater at Guiyang, SW China. *J. Atmos. Chem.* **70**, 269–281 (2013)
- Yang, X., Yao, T.: Different sub-monsoon signals in stable oxygen isotope in daily precipitation to the northeast of the Tibetan Plateau. *Tellus B: Chem. Phys. Meteorol.* **68**, 27922 (2016)
- Yang, Y.J., Liu, J.Q., Di, Y.A., Yang, J., Wen, T.X., Li, Y.W., Shi, Y.Q.: Major ionic composition of precipitation in the Shigatse region, southern Tibetan plateau. *Adv. Mater. Res.* **347–353**, 1005–1011 (2012)
- Yao, T.D., Thompson, L., Yang, W., Yu, W.S., Gao, Y., Guo, X.J., Yang, X.X., Duan, K.Q., Zhao, H.B., Xu, B.Q., Pu, J.C., Lu, A.X., Xiang, Y., Kattel, D.B., Joswiak, D.: Different glacier status with atmospheric circulations in Tibetan Plateau and surroundings. *Nat. Clim. Chang.* **2**, 663–667 (2012)
- Yu, W., Wei, F., Ma, Y., Liu, W., Zhang, Y., Luo, L., Tian, L., Xu, B., Qu, D.: Stable isotope variations in precipitation over Deqin on the southeastern margin of the Tibetan Plateau during different seasons related to various meteorological factors and moisture sources. *Atmos. Res.* **170**, 123–130 (2016)
- Zhang, D.D., Jim, C.Y., Peart, M.R., Shi, C.: Rapid changes of precipitation pH in Qinghai Province, the northeastern Tibetan Plateau. *Sci. Total Environ.* **305**, 241–248 (2003)
- Zhang, Y., Kang, S., Li, C., Cong, Z., Zhang, Q.: Wet deposition of precipitation chemistry during 2005–2009 at a remote site (Nam Co Station) in central Tibetan Plateau. *J. Atmos. Chem.* **69**, 187–200 (2012a)
- Zhang, N., He, Y., Cao, J., Ho, K., Shen, Z.: Long-term trends in chemical composition of precipitation at Lijiang, southeast Tibetan Plateau, southwestern China. *Atmos. Res.* **106**, 50–60 (2012b)
- Zhang, X., Jiang, H., Zhang, Q., Zhang, X.: Chemical characteristics of rainwater in Northeast China, a case study of Dalian. *Atmos. Res.* **116**, 151–160 (2012c)
- Zhang, N., Cao, J., Liu, S., Zhao, Z., Xu, H., Xiao, S.: Chemical composition and sources of PM_{2.5} and TSP collected at Qinghai Lake during summertime. *Atmos. Res.* **138**, 213–222 (2014a)
- Zhang, N., Cao, J., He, Y., Xiao, S.: Chemical composition of rainwater at Lijiang on the southeast Tibetan plateau: influences from various air mass sources. *J. Atmos. Chem.* **71**, 157–174 (2014b)
- Zhang, Q., Shen, Z., Cao, J., Zhang, R., Zhang, L., Huang, R.J., Zheng, C., Wang, L., Liu, S., Xu, H., Zheng, C., Liu, P.: Variations in PM_{2.5}, TSP, BC, and trace gases (NO₂, SO₂, and O₃) between haze and non-haze episodes in winter over Xi'an, China. *Atmos. Environ.* **112**, 64–71 (2015)
- Zhao, M., Li, L., Liu, Z., Chen, B., Huang, J., Cai, J., Deng, S.: Chemical composition and sources of rainwater collected at a semi-rural site in Ya'an, southwestern China. *Atmos. Climate Sci.* **3**, 486 (2013)
- Zongxing, L., Qi, F., Wei, L., Tingting, W., Xiaoyan, G., Zongjie, L., Yan, G., Yanhui, P., Rui, G., Bing, J., Yaoxaun, S., Chuntan, H.: The stable isotope evolution in Shiyi glacier system during the ablation period in the north of Tibetan plateau, China. *Quat. Int.* **380–381**, 262–271 (2015)